CHEMISTRY
A EUROPEAN JOURNAL

DOI: 10.1002/chem.200600182

Hexylene- and Octylene-Bridged Polysilsesquioxane Hybrid Crystals Self-Assembled by Dimeric Building Blocks with Ring Structures

Xufeng Zhou, Sui Yang, Chengzhong Yu,* Zhenhua Li, Xiaoxia Yan, Yong Cao, and Dongyuan Zhao[a]

Abstract: We report the synthesis of novel polysilsesquioxane hybrid crystals prepared from two precursors with hexylene- and octylene-bridged groups. Both crystals are composed of bimolecular rings (18- and 22-membered, respectively) formed by one-step condensation of two hydrolyzed monomers. The hydrogen bonds between silanol groups and the weak van der Waal's interactions between alkyl chains link the large rings as building blocks together into self-assembled, three-dimensional molecular crystalline structures. The precise control of the sol–gel process is considered to be the crucial factor in fabricating flexible long alkyl chains into an ordered stacking. These contributions extend the understanding of the sol–gel chemistry of polysilsesquioxanes.

Keywords: alkyl chains · hybrid crystals · polysilsesquioxane · self-assembly · sol–gel processes

Introduction

Organic–inorganic hybrid materials have attracted much attention in material science due to their rich properties, derived from both the organic and inorganic moieties, and their many applications in modern society.[1] Polysilsesquioxanes are a family of hybrids that have been investigated for many years because of their advantages in various applications. A new kind of polysilsesquioxane named bridged polysilsesquioxane, in which the organic group acts as a bridge linking two Si atoms together, gives the opportunity to obtain hybrids with uniformly mixed organic and inorganic moieties at the molecular level. Accessible monomers include two or more alkoxysilyl groups or silyl chlorides as inorganic precursors and the organic bridge group may vary from alkane, alkene, alkyne, aromatic, to functionalized organic structures.[2] The large variety of the precursors imparts various properties to the obtained hybrids, making them good candidates for surface modifiers, coatings, catalysts, and membrane materials.[2a,3]

By introducing different bridge groups to precursors, it is possible for scientists to explore new structures of polysilsesquioxanes. Although the synthesis of bridged polysilsesquioxanes usually adopts a sol–gel process similar to that of amorphous silica, some interesting structures other than amorphous hybrids can be obtained. In some reports, products with local ordering are attained. Organic groups with strong interactions, such as π–π stacking or hydrogen bonds, and/or with rigid backbones, can be regularly arranged in local areas during the sol–gel reaction, enduing the hybrids with anisotropy.[4] Some research groups have also reported the preparation of bridged polysilsesquioxanes with long-range ordering,[5] in some cases crystals with flakelike morphology are formed.[5b,d] In the latter two cases,[5b,d] X-ray diffraction (XRD) patterns and transmission electron microscopy (TEM) images revealed the lamellar structure of the hybrids. The hydrogen bonds among urea groups in the organic bridge and π–π stacking of benzene groups was believed to be the driving force for the crystal formation. However, the ^{29}Si NMR analysis gave signals of silicon atoms with different condensation degrees, suggesting imperfect atomic ordering in these hybrids. This is attributed to difficulties in the accurate control of the sol–gel reaction of bridged silsesquioxane precursors. In rare cases, the condensation can be restrained under biphasic reaction systems, leading to organo(bis-silanetriol)[6] or organo(bis-silanediol)[7] crystals consisting of completely hydrolyzed, but not condensed, monomers with short and rigid phenyl bridge groups.

[a] X. Zhou, S. Yang, Prof. C. Yu, Z. Li, X. Yan, Prof. Y. Cao, Prof. D. Zhao
Department of Chemistry and Shanghai Key Laboratory of Molecular Catalysis and Innovative Materials, Fudan University
Shanghai 200433 (P. R. China)
Fax: (+86) 21-6564-1740
E-mail: czyu@fudan.edu.cn

Until now, all the self-organized bridged polysilsesquioxanes reported were synthesized from precursors with organic groups that may generate strong interactions and/or rigidity. Hybrids derived from precursors with flexible alkylene $[(CH_2)_n]$-bridged groups were all reported to be amorphous.[8] Systematic studies revealed a high dependence of the sol–gel behavior of such precursors on the length of the alkyl chain, that is, the number of n. Monomers of $n \leq 4$ exhibit a pronounced tendency to undergo rapid intra- or intermolecular (bimolecular) cyclization (commonly seven- or eight-membered rings), which greatly slows down the gelation. In contrast, monomers with longer alkyl chains experience a normal sol–gel process.[2b,9] Nevertheless, in all cases, amorphous gels or precipitates are obtained due to the flexibility and weak intermolecular interaction of the alkyl chains.

Here, we report the synthesis and characterization of silsesquioxane hybrid crystals prepared from two precursors with hexylene- and octylene-bridged groups, respectively. To our knowledge, this is the first report that hybrid polysilsesquioxane crystals are assembled from precursors with flexible long alkyl chains. Both crystals are composed of bimolecular rings (18- and 22-membered, respectively) formed by one-step condensation of two hydrolyzed monomers. Hydrogen bonds between silanol groups and weak van der Waal's interactions between alkyl chains link the rings together into three-dimensional molecular crystalline structures. The precise control of the sol–gel process is considered to be the crucial factor in fabricating flexible long alkyl chains into an ordered stacking.

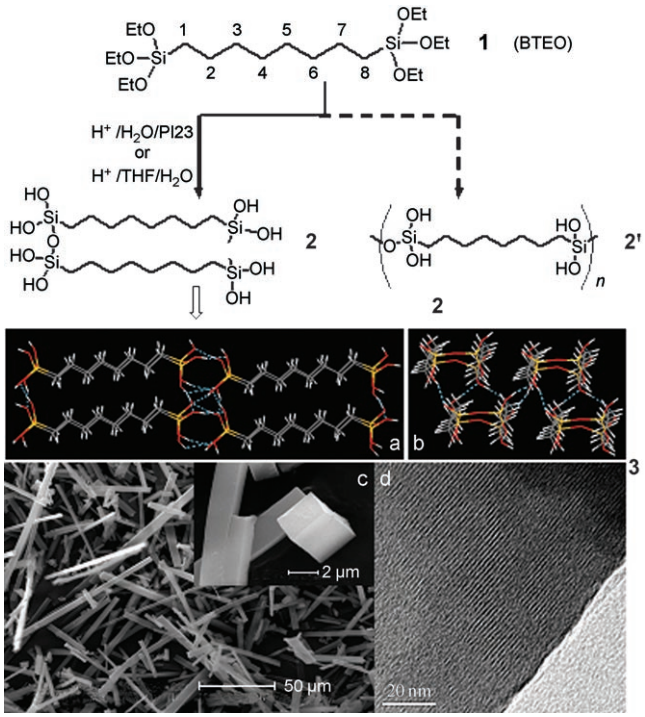

Scheme 1. Top: Reaction process from the precursor (**1**) to possible building blocks **2** (cyclic dimer) or **2′** (one-dimensional chain), and the final crystal structure (**3**) constituted from **2**. Bottom: a) and b) Theoretically calculated (010) and (001) surfaces, respectively, of **3**. Si, O, C, H atoms are yellow, red, gray, and white, respectively. Blue dashed lines represent some selected hydrogen bonds. c) and d) SEM and TEM images, respectively, of **3**.

Results

Octylene-bridged polysilsesquioxane crystals: Octylene-bridged polysilsesquioxane hybrid crystals can be obtained either from aqueous solution with the addition of a nonionic triblock copolymer P123 (poly[(ethylene oxide)-*b*-(propylene oxide)-*b*-(ethylene oxide)], $EO_{20}PO_{70}EO_{20}$) or from a tetrahydrofuran (THF) system in the absence of surfactant (Scheme 1). The following characterizations are based on the samples from the first case. The hydrolysis and condensation of the monomer bis(triethoxysilyl)octane (**1**) (BTEO) leads to white precipitate (**3**), which is transparent under the optical microscope. Scanning electron microscopy (SEM) images (Scheme 1c) show high yield, needlelike crystals with parallelogram facets almost vertical to the long axis. The length of the crystals is in the region of around 100 μm, and the width and thickness range from 2–5 and 1–2 μm, respectively. The TEM image (Scheme 1d) of the sample reveals further the internal ordering of the crystals. The highly ordered alternation of white and black stripes is due to the different electron densities between silicon and carbon atoms. The periodicity of the pattern, that is, the distance between two neighbouring white or black stripes is measured to be ~16 Å.

The high crystallinity of the product **3** was observed further by powder XRD analysis. At least 16 peaks are well resolved at $2\theta < 30°$ (Figure 1). The d-spacing calculated from the first peak ($2\theta = 5.34°$) is 16.5 Å, very close to the periodicity observed in the TEM image (16 Å). However, the endeavour to the index of the XRD peaks and further resolution of the crystal structures by using powder XRD patterns was not successful. In addition, the crystals of **3** that we prepared are too small in width and thickness for them to be analyzed by single-crystal X-ray diffraction. Therefore, other chemical-analysis techniques were applied to determine the composition and structure of hybrid **3**.

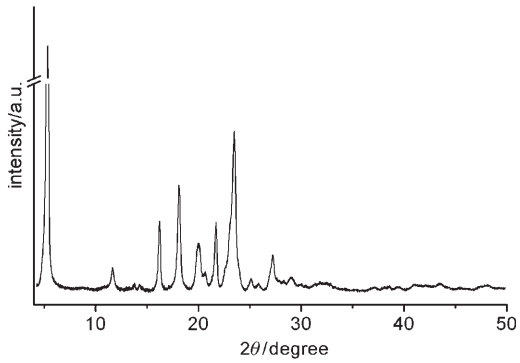

Figure 1. Powder X-ray diffraction pattern of **3**.

The solution- ([D_6]DMSO as the solvent) and solid-state ^{29}Si NMR spectra of **3** (Figure 2a and c) show only one sharp peak centered at −50.7 and −52.8 ppm, respectively, which corresponds to the Si atom of T^1 resonance, indicating

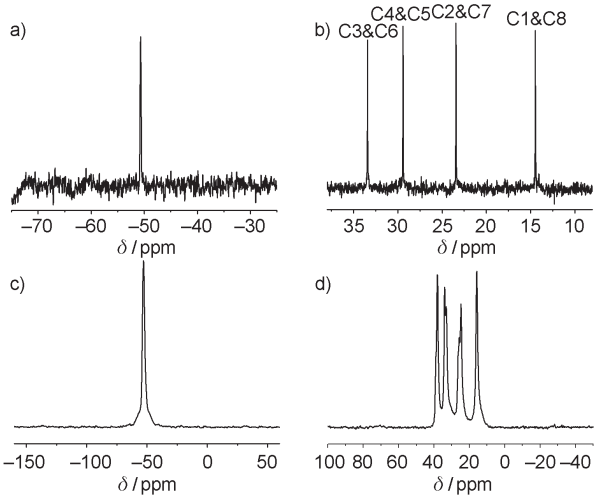

Figure 2. a) ^{29}Si NMR and b) ^{13}C NMR spectra of **3** dissolved in [D_6]DMSO. c) Solid-state ^{29}Si MAS-NMR and d) solid-state ^{13}C MAS-NMR spectra of **3**.

that **3** consists predominantly of geminal silanol structure, $(HO)_2RSi(OSi)$. The lack of Q signals reveals the preservation of the Si−C bond throughout the reaction. Careful analysis of the T^1 signal in the solid-state NMR spectrum shows that the peak has an asymmetric shape, which may be an overlap of two peaks. A detailed explanation follows in the comparison with hexylene-bridged hybrids (see Figure 7). Quantitative ^{1}H NMR measurement (data not shown) reveals that the population ratio of oxygen-bonded hydrogen atoms (5.83 ppm) to carbon-bonded ones (0.41, 1.23, and 1.34 ppm) in **3** is one quarter of the integrated peak-area ratios, confirming further the existence of two hydroxyl groups bonded to each silicon atom.

The NMR results are also validated by elemental analysis. The measured content of C 38.06, H 7.98, and Si 23.5% (by the inductively coupled plasma method, ICP) indicates the formula of $[(CH_2)_8Si_2(OH)_4O]$ (calculated elemental content is C 38.10, H 7.94, and Si 22.2%). Two possible structure units in accordance with this formula are then presented, as shown in Scheme 1, **2** and **2′**, a cyclic dimer with a molecular weight of 504 and a long one-dimensional chain with a much higher molecular weight. The ESI-MS analysis of **3** (dissolved in DMSO) gives three main signals at $m/z = 527$ $[M+Na]^+$ (504+23), 469 $[M-(H_2O+OH)]^+$ (504–35), and 451 $[M-(2H_2O+OH)]^+$ (504−53), supporting the existence of **2** and excluding **2′**. The signals at $m/z = 469$ and 451 are probably attributed to the dehydration of the dimers, which may occur easily for molecules with many hydroxyl groups under ionization.

To determine the spatial structure of the dimer **2** in the crystal **3**, especially the conformation of the octylene chain, ^{13}C NMR and FTIR spectroscopy were performed. Figure 2b shows the solution-state ^{13}C NMR spectra of **3** dissolved in [D_6]DMSO. The absence of the resonance of carbon atoms linked to oxygen atoms suggests the complete hydrolysis of the precursor **1**. The four sharp peaks observed correspond to four groups of carbon atoms in the octylene chain, based on their symmetry. The assignment of these peaks, which is analogous to that of octane, is displayed in Figure 2. The chemical shifts of C1 and C8 are at a higher field than their counterparts in octane because the electronegativity of a Si atom is lower than that of a C atom. Similarly, there are also four groups of peaks in the solid-state ^{13}C NMR spectrum of **3** (Figure 2d), which has the same assignment as that in Figure 2b, although two features that are distinct from the solution-state NMR spectra are observed. Firstly, the two peaks originally located at 23.5 (C2 and C7) and 29.4 ppm (C4 and C5) in the solution-state NMR spectra are both split into two close peaks at 24.8; 25.7, and 33.1; 34.0 ppm, respectively. Secondly, the chemical shifts of the same group of carbon atoms in the solid state all move to lower field. Interestingly, the extents of the shifts are different for the four groups of carbon atoms. C1 and C8, linked to the Si atoms, have the smallest shift of 1.3 ppm; C2 and C7, next adjacent to the Si atoms, show a relatively small shift of ~1.8 ppm; the other four atoms in the middle of the octylene chain possess the most distinct shift of ~4.2 (C4 and C5) and 4.7 ppm (C3 and C6). In the study of self-assembled monolayers, a downfield shift (~4 ppm) of the resonances of interior carbons relative to the corresponding values for a liquid-phase alkane with equilibrium populations of *trans* and *gauche* conformations was taken as evidence for all-*trans* conformations of the chains.[10] Comparison of our own data with the literature indicates that the octylene spacers in the solid state are in all-*trans* conformations, rather than flexible alkyl chains when **3** is dissolved. The sharpness of the peaks (full-width at half-maximum (fwhm) of ~1 ppm) also suggests the crystalline form of the material. The split of the resonances might be attributed to the high degree of organization of the solid sample, which induces different conformations or environments of different carbon atoms.

The FTIR spectrum of **3** is shown in Figure 3. The broad band centered at 3250 cm^{-1} is assigned to the stretching vibration of silanol groups (SiO−H). The shift of the peak position from 3750 cm^{-1} (assigned to the vibration of isolated silanol) to the lower wavenumber indicates that the silanol groups in **3** are hydrogen bonded. The existence of silanol groups is also proved by the singlet at 906 cm^{-1}, which is assigned to the Si−OH stretching mode. The band at 1136 cm^{-1} is attributed to Si−O−Si stretching mode. Bands centered at 2920 and 2854 cm^{-1} are assigned to the symmetric and antisymmetric stretching-vibration mode, respectively, of the C−H in the methylene unit. The narrow fwhm values (15 and 23 cm^{-1}) of these two peaks confirm the high crystallinity of the product, consistent with the similar observation in the crystalline alkylsiloxanes of longer alkyl chains (C18).[10] The peak of 1464 cm^{-1} corresponds to a CH_2 scis-

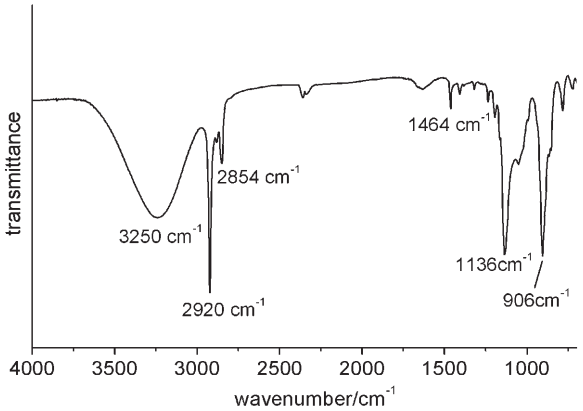

Figure 3. FTIR spectrum of **3**.

soring-deformation mode. The fwhm of 9 cm^{-1} also suggests the ordering of the carbon chains with all-*trans* conformation in the solid. Several bands are observed between 1165 and 1385 cm^{-1}, which is attributed to coupled CH_2 wag modes. The interband spacing in this area can be used to calculate the number of carbon atoms in an all-*trans* conformational structure.[10] Because of the limitation of the band numbers, we calculated the average spacing from three peaks. The value of 35.5 cm^{-1} approximates the theoretical value of 36.2 cm^{-1} from an all-*trans* octylene chain. The all-*trans* conformation of the octylene chain is also evidenced by the Raman spectrum (Figure 4). The intensity ratio of the methylene asymmetric vibration band (2883 cm^{-1}) to the symmetric vibration band (2862 cm^{-1}) is calculated to be 1.9 in our system, close to the value of 2.0 reported in a crystalline solid.[11]

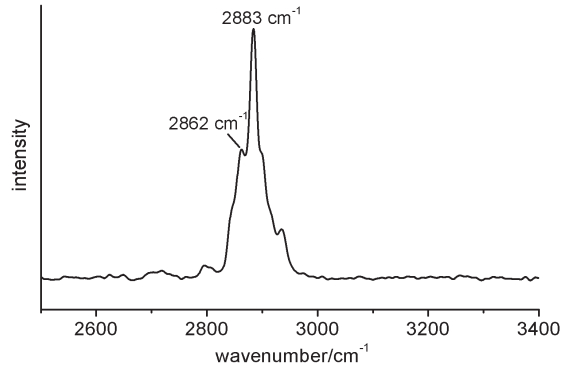

Figure 4. Raman spectrum of **3**.

Because no suitable crystals for single-crystal X-ray diffraction analysis were available, we performed theoretical calculations to support further our speculation of the dimer and to gain some information of the spatial stacking with the Material Studio (MS) software package (Accelrys).[12] The optimized crystal structure of **3** has cell parameters of $a=4.918$, $b=8.030$, $c=16.040$ Å, agreeing well with the largest *d*-spacing of 16.5 Å measured from the XRD pattern. Scheme 1a and b represent the (010) and (001) surfaces, respectively, of **3**. Hydrogen bonds among **2** (for clarity, only some of the hydrogen bonds are shown in Scheme 1a and b by blue dashed lines) as well as the London dispersion among the octylene chains link such building blocks together and auto-organize them further into three-dimensional hybrid molecular crystal **3**. Frequency analysis indicates that **3** has no vibration higher than 3500 cm^{-1}, consistent with the experimental IR spectrum. The same calculation on the basis of **2′** as the structure unit gives the lattice parameter *c* of 14.62 Å and a vibration frequency at 3682 cm^{-1}, both disagreeing with our experimental results. We also calculated the energy change from bis(trihydroxysilyl)octane (completely hydrolyzed product of **1**) to crystal **3** via **2** as building blocks or a one-dimensional structured solid constructed from **2′** at 0 K with zero-point vibrational energy correction. The result shows that the formation of **3** is by 3.9 kcal mol^{-1} energetically more favorable, constituting a thermodynamic explanation for the formation of **3** via **2** as building blocks. The outcome of this calculation validates further our preceding deduction of structure **3** from the experimental results.

Hexylene-bridged polysilsesquioxane crystals: The precipitates from hydrolysis and condensation of bis(triethoxysilyl)-hexane (BTEH) under identical experimental conditions to that of bis(triethoxysilyl)octane also have high crystallinity. The following data is from the sample synthesized in the THF system. The SEM and TEM images (Figure 5) show identical needlelike morphology and ordered internal structure, respectively.

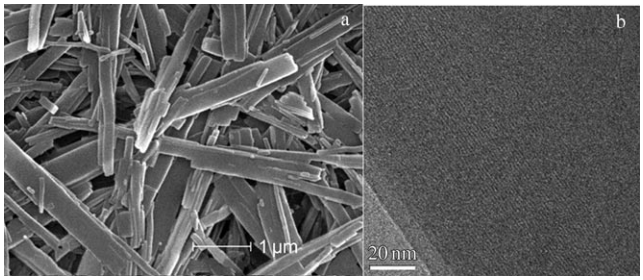

Figure 5. a) SEM and b) TEM images of crystalline hybrids synthesized from BTEH.

The XRD pattern of the hexylene-bridged hybrid is shown in Figure 6. The first peak corresponds to the *d*-spacing of 14.2 Å, also similar to the distance calculated from the TEM image (Figure 5b). The *d*-spacing is 2.3 Å shorter than that of octylene-bridged hybrids, close to the difference in length of octylene and hexylene chains if both are in the all-*trans* conformation. Meanwhile, several peaks at $2\theta=$ 11.6, 21.7, 23.4, and 27.3° appear in both XRD patterns, suggesting some structural similarity of the two hybrid crystals. The FTIR spectrums of the two crystals are almost identical, suggesting the all-*trans* form of the hexylene group in the hybrid (data not shown).

The solid-state ^{13}C NMR spectrum gives three sets of peaks, the assignments of which are shown in Figure 7a. The

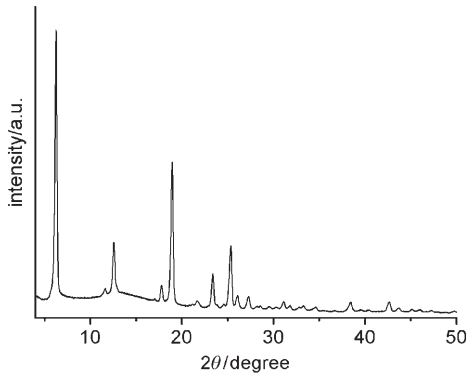

Figure 6. Powder XRD pattern of hybrid crystal synthesized from BTEH.

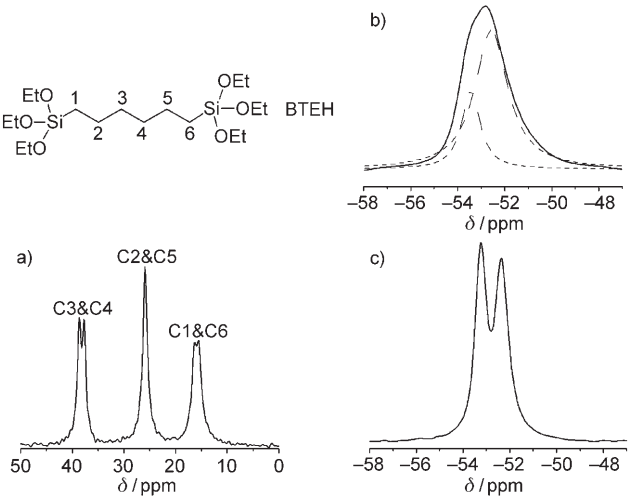

Figure 7. a) Solid-state ^{13}C NMR spectra of hybrid crystals prepared from BTEH, b) solid-state ^{29}Si NMR spectra of crystals prepared from BTEO (dashed lines represent fitted peaks), and c) solid-state ^{29}Si NMR spectra of crystals prepared from BTEH.

peak movement similar to that in the case of octylene-bridged polysilsesquioxane crystals from liquid to solid state and the peak splits are also observed. The sharpness of the peaks (fwhm ~1 ppm) also implies the crystalline form of the material. Interestingly, the solid-state NMR spectrum of ^{29}Si (Figure 7c) has two adjacent signals at −53.2 and −52.4 ppm. Both peaks should be assigned to T^1 signals of Si. The split of the peak is believed to be the result of the crystallization. Actually, as previously mentioned, the ^{29}Si NMR signal of octylene-bridged hybrids (Figure 7b) is an overlap of two peaks. The multipeak fit decomposes the signal into two peaks, centered at −53.6 and −52.8 ppm. Although the peak positions of the two samples are slightly different, the chemical-shift between the two peaks in both cases is 0.8 ppm, which may suggest the structural comparability of the two crystals. Elemental analysis revealed the content of C, H, and Si to be 33.43, 7.15, and 21% (by ICP), respectively. An ESI-MS spectrum shows two main signals at $m/z = 471$ $[M+Na]^+$ and 413 $[M-(H_2O+OH)]^+$, indicating a formula of $[(CH_2)_6Si_2(OH)_4O]_2$ (molecular weight: 448, calculated elemental content is C 32.1, H 7.14, and Si 25%). Based on all these results, it is concluded that the hexylene-bridged hybrid crystal has a similar molecular crystal structure to that of **3**, with a slightly different 18-membered dimeric ring as the building block. Due to the parallelogram shape of the dimer, it is inferred that the silicon atoms at the four corners should have some different chemical environment if the cyclic dimers stack together, that is, two Si on one diagonal have the same environment, which is slightly different to that of the other two located at the other diagonal, leading to the split in the solid-state ^{29}Si NMR spectra.

Discussion

The porosity, condensation degree, and other physicochemical properties of bridged polysilsesquioxanes are kinetically controlled and can be adjusted within a wide range, not only in the cases of alkylene-bridged precursors, but also among all other kinds of bridged polysilsesquioxanes. The hydrolysis and condensation of organosilica species is different from that of pure silica and are commonly known as induction and steric effects.[13] By varying the experimental conditions of hydrolysis and condensation, such as the concentration of precursors, catalysts, synthetic temperature, pH value of the reaction system, and solvent, the final structures and physicochemical properties of the products can be changed.[8b,14] In previous reports, the bridged polysilsesquioxanes with ordered structures were usually synthesized under conditions that may decrease the hydrolysis and condensation rate, for example, by utilizing a low concentration of precursors or by using inert solvents. Importantly, in previous reports, use of the same precursors as in our synthesis resulted in only amorphous materials.[8b,9c]

The unusual results of our experiment compared with the literature are attributed mainly to the controlled reaction conditions. With six reaction sites per molecule and with the induction effect of the alkyl chain, the precursor BTEO or BTEH is easily hydrolyzed and tends to be polycondensed under normal acid- or base-catalyzed conditions, leading to amorphous bridged polysilsequioxanes. In our synthesis, use of surfactant P123 or dilution of the reactants with a large quantity of organic solvent THF (0.1 g of BTEO or BTMH in 50 mL of THF) greatly slows down the sol–gel reaction, which favors the formation of dimers by a one-step bimolecular condensation rather than polymerization. As soon as the cyclic dimers formed, further condensation was energetically unfavorable because of the large steric effect, similar to that observed in the formation of polysilsesquioxanes bridged by short alkyl chains in which a cyclic intermediate also forms.[9]

Relative to the reaction conditions in THF solution, the concentration of precursors is ~10 times higher in the case of aqueous synthesis with P123, and the temperature is also higher (from 5 to 40 °C); moreover, a large quantity of reactive water exists. The formation of molecular crystals is at-

tributed to the existence of block copolymer P123 in the system. Nonionic block copolymer P123 is commonly used as a template in the self-assembly of ordered mesoporous silica and organosilica.[15] Other surfactants can also be used to synthesize ordered mesoporous bridged polysilsesquioxane[16] or even mesoporous organosilica with crystallized walls.[17] However, N_2 sorption analysis reveals that all the molecular crystals obtained in our synthesis are dense materials (data not shown), and other characterization results (e.g., IR, NMR) show that the block copolymer P123 does not exist in the crystals. Clearly, the role of P123 cannot be viewed as a supramolecular template as in the formation of mesoporous materials. We propose that the protonated hydrophilic block of poly(ethylene oxide) (PEO) under acidic conditions might have relatively strong interactions with silanol groups through hydrogen bonds or electrostatic interactions. Therefore, the hydrolyzed BTEO or BTEH molecules, which have plenty of silanol groups, will interact preferentially with P123 molecules. In the presence of large P123 molecules, further condensation is greatly inhibited, due to the steric limitation. Dimers with one-step condensation are favorable in solution and self-assemble further into molecular crystals.

Other factors, such as the acidity and temperature, are also important for the formation of molecular crystals. In the aqueous system, pure crystals with needlelike morphology can be obtained only under the acidity of 0.3 M HCl with the help of P123. Increasing acidity (0.5–1 M HCl) accelerates the sol–gel reaction rate and induces amorphous hybrids along with crystals. Only amorphous products are obtained as the HCl concentration reaches 2 M. In the case of the THF system, the low temperature (5 °C), as well as the low concentration of the precursors, is important to successfully synthesize hybrid crystals.

The influence of the length of the alkyl chain in $[(CH_2)_n]$-bridged groups should be considered further. The all-*trans* conformation of long alkyl groups is energetically more favourable if they are closely packed, as has been proved in the cases of surface self-assembly of *n*-alkylsiloxane.[10,18] However, for the formation of molecular crystals from bis(triethoxysilyl)alkane precursors, the effect of n is still an open challenge. Preliminary theoretical calculations suggest that the formation of molecular crystals via dimeric building blocks is favorable in the region of $5 \leq n \leq 12$. For longer chains, say $n > 12$, there would be many conformations in the solution. Formation of a dimer requires only a few straight-chain conformations. From the point of view of entropy change, the formation of a dimer may not be preferred. Further experiments and calculations are necessary to elucidate these matters.

Conclusion

We have successfully synthesized bridged polysilsesquioxane crystals with flexible long alkyl chains (octylene and hexylene) as the bridged group. This contrasts with the current assumption that the use this family of precursors induces only amorphous polysilsesquioxanes. Physicochemical characterization and theoretical calculations suggest that the crystals consist of large cyclic dimers that derive from a one-step bimolecular condensation of completely hydrolyzed precursor molecules. The hydrogen bonds among geminal silanol groups in the dimers and the weak van der Waal's interactions among alkyl chains link the dimers regularly into three-dimensional molecular crystals. These contributions extend the understanding of the sol–gel chemistry of polysilsesquioxanes and provide an alternative means to synthesize bridged polysilsesquioxane crystals possessing other flexible organic groups with various functions.

Experimental Section

Bis(triethoxysilyl)octane and bis(triethoxysilyl)hexane were purchased from Gelest (97%). Triblock poly[(ethylene oxide)-*b*-(propylene oxide)-*b*-(ethylene oxide)] copolymer $EO_{20}PO_{70}EO_{20}$ (denoted P123, $M_r = 5800$) was purchased from Aldrich. All chemicals were used as received without purification. In a typical aqueous synthetic process, P123 (0.3 g) was dissolved in HCl (0.2 M, 20 mL). Bis(triethoxysilyl)octane (0.4 g) or bis(triethoxysilyl)hexane (0.4 g) was added to the solution and this was stirred for 10 min. After keeping the solution static for 1 d at 40 °C, the white precipitant obtained was filtrated, washed with water and ethanol, and dried in air. In a typical organic-solvent synthesis, bis(triethoxysilyl)octane (0.1 g) or bis (triethoxysilyl)hexane (0.1 g) was added to a solution of THF (50 mL) and HCl (0.05 M, 1 mL) at 5 °C. The resultant mixture was stirred at the same temperature for 1 h and was kept static at the same temperature for 1 d. The product was filtered, washed with water and ethanol, and dried in air.

XRD patterns were recorded by using a Bruker D4 Endeavor diffractometer with $Cu_{K\alpha}$ radiation at a working voltage of 40 kV and a working current of 40 mA. TEM images were obtained by using a JEOL2010 transmission electron microscope with an acceleration voltage of 200 kV. SEM images were recorded by using a Philip XL30 scanning electron microscope operated at 20 kV and the samples were coated with gold. The FTIR spectra were collected by using a Nicolet FTIR 360 spectroscope (KBr method) at the scanning rate of 2 cm^{-1} per step. Raman spectra was recorded by using a J-Y LabRam-IB spectrometer using 3 mW of 632.8 nm radiation from a He–Ne laser. Cross-polarization magic-angle spinning (CP-MAS) ^{13}C NMR spectra and single-pulse MAS ^{29}Si NMR spectra with proton decoupling were recorded by using a Bruker DSX 300 and a Bruker DSX 500 for solid- and solution-state NMR, respectively. ESI-MS analysis was performed by using an Agilent LC-MSD SL spectrometer with the capillary voltage of 3850 V.

Calculation method: The unit cells of the crystals were optimized with the discovery module by using compass force field. The structures were refined further by using the DMol3 program with the GGA PW91 density functional method in combination with a numerical DNP basis set.

Acknowledgements

This work was supported by the National Science Foundations of China (20301004, 20421303), the State Key Research Program (2004CB217800), the Shanghai Science Committee (03QF14002), and FANEDD (200423).

[1] a) P. Judeinstein, C. Sanchez, *J. Mater. Chem.* **1996**, *6*, 511–525; b) C. Sanchez, B. Julian, P. Belleville, M. Popall, *J. Mater. Chem.* **2005**, *15*, 3559–3592.

[2] a) H. W. Oviatt, K. J. Shea, S. Kalluri, Y. Q. Shi, W. H. Steier, L. R. Dalton, *Chem. Mater.* **1995**, *7*, 493–498; b) D. A. Loy, J. P. Carpenter, S. A. Yamanaka, M. D. McClain, J. Greaves, S. Hobson, K. J. Shea, *Chem. Mater.* **1998**, *10*, 4129–4140; c) B. Boury, R. J. P. Corriu, V. Le Strat, *Chem. Mater.* **1999**, *11*, 2796–2803; d) B. Boury, R. J. P. Corriu, *Adv. Mater.* **2000**, *12*, 989–992; e) P. Chevalier, R. J. P. Corriu, P. Delord, J. J. E. Moreau, M. W. C. Man, *New J. Chem.* **1998**, *22*, 423–433; f) K. J. Shea, D. A. Loy, O. Webster, *J. Am. Chem. Soc.* **1992**, *114*, 6700–6710; g) J. P. Bezombes, C. Chuit, R. J. P. Corriu, C. Reye, *J. Mater. Chem.* **1999**, *9*, 1727–1734; h) R. J. P. Corriu, C. Hoarau, A. Mehdi, C. Reye, *Chem. Commun.* **2000**, 71–72; i) D. A. Loy, J. V. Beach, B. M. Baugher, R. A. Assink, K. J. Shea, J. Tran, J. H. Small, *Chem. Mater.* **1999**, *11*, 3333–3341; j) M. Jurado-Gonzalez, D. L. Ou, B. Ormsby, A. C. Sullivan, J. R. H. Wilson, *Chem. Commun.* **2001**, 67–68.

[3] a) D. A. Loy, K. J. Shea, *Chem. Rev.* **1995**, *95*, 1431–1442; b) K. J. Shea, D. A. Loy, *Chem. Mater.* **2001**, *13*, 3306–3319; c) J. J. E. Moreau, M. W. C. Man, *Coord. Chem. Rev.* **1998**, *180*, 1073–1084; d) E. Lindner, T. Schneller, F. Auer, H. A. Mayer, *Angew. Chem.* **1999**, *111*, 2288–2309; *Angew. Chem. Int. Ed.* **1999**, *38*, 2155–2174; e) N. G. Liu, K. Yu, B. Smarsly, D. R. Dunphy, Y. B. Jiang, C. J. Brinker, *J. Am. Chem. Soc.* **2002**, *124*, 14540–14541.

[4] a) B. Boury, R. J. P. Corriu, *Chem. Commun.* **2002**, 795–802; b) B. Boury, F. Ben, R. J. P. Corriu, P. Delord, M. Nobili, *Chem. Mater.* **2002**, *14*, 730–738; c) G. Cerveau, R. J. P. Corriu, F. Lerouge, N. Bellec, D. Lorcy, M. Nobili, *Chem. Commun.* **2004**, 396–397.

[5] a) B. Boury, F. Ben, R. J. P. Corriu, *Angew. Chem.* **2001**, *113*, 2946–2948; *Angew. Chem. Int. Ed.* **2001**, *40*, 2853–2856; b) J. J. E. Moreau, L. Vellutini, M. W. C. Man, C. Bied, J. L. Bantignies, P. Dieudonne, J. L. Sauvajol, *J. Am. Chem. Soc.* **2001**, *123*, 7957–7958; c) H. Muramatsu, R. Corriu, B. Boury, *J. Am. Chem. Soc.* **2003**, *125*, 854–855; d) J. J. E. Moreau, B. P. Pichon, M. W. C. Man, C. Bied, H. Pritzkow, J. L. Bantignies, P. Dieudonne, J. L. Sauvajol, *Angew. Chem.* **2004**, *116*, 205–208; *Angew. Chem. Int. Ed.* **2004**, *43*, 203–206; e) K. Okamoto, Y. Goto, S. Inagaki, *J. Mater. Chem.* **2005**, *15*, 4136–4140.

[6] G. Cerveau, R. J. P. Corriu, B. Dabiens, J. Le Bideau, *Angew. Chem.* **2000**, *112*, 4707–4711; *Angew. Chem. Int. Ed.* **2000**, *39*, 4533–4537.

[7] F. Carre, G. Cerveau, R. J. P. Corriu, B. Dabiens, *J. Organomet. Chem.* **2001**, *624*, 354–358.

[8] a) D. A. Loy, G. M. Jamison, B. M. Baugher, E. M. Russick, R. A. Assink, S. Prabakar, K. J. Shea, *J. Non-Cryst. Solids* **1995**, *186*, 44–53; b) D. A. Loy, B. Mather, A. R. Straumanis, C. Baugher, D. A. Schneider, A. Sanchez, K. J. Shea, *Chem. Mater.* **2004**, *16*, 2041–2043.

[9] a) D. A. Loy, J. P. Carpenter, S. A. Myers, R. A. Assink, J. H. Small, J. Greaves, K. J. Shea, *J. Am. Chem. Soc.* **1996**, *118*, 8501–8502; b) D. A. Loy, J. P. Carpenter, T. M. Alam, R. Shaltout, P. K. Dorhout, J. Greaves, J. H. Small, K. J. Shea, *J. Am. Chem. Soc.* **1999**, *121*, 5413–5425; c) K. J. Shea, D. A. Loy, *Acc. Chem. Res.* **2001**, *34*, 707–716.

[10] A. N. Parikh, M. A. Schivley, E. Koo, K. Seshadri, D. Aurentz, K. Mueller, D. L. Allara, *J. Am. Chem. Soc.* **1997**, *119*, 3135–3143.

[11] W. R. Thompson, J. E. Pemberton, *Langmuir* **1995**, *11*, 1720–1725.

[12] *Accelrys*, *Materials Studio 3.0*, *Accelrys*, *San Diego*, **2004**.

[13] C. J. Brinker, G. W. Scherer, *Sol–Gel Science: The Physics and Chemistry of Sol–Gel Processing*, Academic Press, Boston, **1990**.

[14] a) G. Cerveau, R. J. P. Corriu, C. Fischmeister-Lepeytre, *J. Mater. Chem.* **1999**, *9*, 1149–1154; b) G. A. Cerveau, R. J. P. Corriu, E. Framery, *J. Mater. Chem.* **2000**, *10*, 1617–1622; c) G. Cerveau, S. Chappellet, R. J. P. Corriu, *J. Mater. Chem.* **2003**, *13*, 2885–2889.

[15] a) D. Y. Zhao, J. L. Feng, Q. S. Huo, N. Melosh, G. H. Fredrickson, B. F. Chmelka, G. D. Stucky, *Science* **1998**, *279*, 548–552; b) O. Muth, C. Schellbach, M. Froba, *Chem. Commun.* **2001**, 2032–2033; c) X. Y. Bao, X. S. Zhao, X. Li, P. A. Chia, J. Li, *J. Phys. Chem. B* **2004**, *108*, 4684–4689.

[16] a) T. Asefa, M. J. MacLachan, N. Coombs, G. A. Ozin, *Nature* **1999**, *402*, 867–871; b) S. Inagaki, S. Guan, Y. Fukushima, T. Ohsuna, O. Terasaki, *J. Am. Chem. Soc.* **1999**, *121*, 9611–9614; c) B. J. Melde, B. T. Holland, C. F. Blanford, A. Stein, *Chem. Mater.* **1999**, *11*, 3302–3308; d) G. Soler-Illia, C. Sanchez, B. Lebeau, J. Patarin, *Chem. Rev.* **2002**, *102*, 4093–4138; e) B. Hatton, K. Landskron, W. Whitnall, D. Perovic, G. A. Ozin, *Acc. Chem. Res.* **2005**, *38*, 305–312.

[17] a) S. Inagaki, S. Guan, T. Ohsuna, O. Terasaki, *Nature* **2002**, *416*, 304–307; b) M. P. Kapoor, Q. H. Yang, S. Inagaki, *J. Am. Chem. Soc.* **2002**, *124*, 15176–15177; c) K. Okamoto, M. P. Kapoor, S. Inagaki, *Chem. Commun.* **2005**, 1423–1425; d) A. Sayari, W. H. Wang, *J. Am. Chem. Soc.* **2005**, *127*, 12194–12195.

[18] A. Baptiste, A. Gibaud, J. F. Bardeau, K. Wen, R. Maoz, J. Sagiv, B. M. Ocko, *Langmuir* **2002**, *18*, 3916–3922.

Received: February 9, 2006
Published online: August 22, 2006

